Vol. 74: 15–30, 2017
https://doi.org/10.3354/cr01487

CLIMATE RESEARCH
Clim Res

Published online October 16

A climatology of convective available potential energy in the Mediterranean region

C. J. Lolis*

Laboratory of Meteorology, Department of Physics, University of Ioannina, 45110 Ioannina, Greece

ABSTRACT: The climatic characteristics of convective available potential energy (CAPE) over the Mediterranean region are studied. The data used are daily grid point (1° × 1°) values of CAPE for the period 1979–2015, obtained from the ERA-Interim data base. The main modes of the intra-annual variation and the spatial distribution of CAPE are revealed using a multivariate data reduction technique. Four main modes of intra-annual variation are found, which correspond to specific Mediterranean sub-regions: (1) the continental areas north of the Mediterranean Sea, presenting a maximum in summer and a minimum in winter; (2) the southern Mediterranean Sea and NW Africa, showing a maximum in early autumn; (3) the northern Egyptian coasts, showing a maximum in October; and (4) the continental areas of Asia Minor, characterized by maxima in late spring and early autumn and minima in winter and summer. Four main modes of spatial distribution are found, one for each season: (i) the autumn pattern presents a maximum over the southern Mediterranean Sea; (ii) the winter pattern is characterized by highest CAPE values over the NE Mediterranean Sea; (iii) the spring pattern presents maxima over the inland areas north of the Mediterranean Sea, Asia Minor and the Atlas mountains; and (iv) the summer pattern is characterized by a maximum over the Adriatic Sea. Finally, the linear trends of CAPE during the period 1979–2015 show a significant increase in many parts of the Eastern Mediterranean region, especially in the warm period.

KEY WORDS: Convective available potential energy · CAPE · Mediterranean Sea · Seasonal variability · Spatial variability · Trends

1. INTRODUCTION

The convective available potential energy (CAPE) is the amount of energy per unit mass which is available for convection. It is a significant meteorological quantity connected to the static instability of the atmosphere, which is generally responsible for heavy precipitation, thunderstorms, tornados, waterspouts and other violent atmospheric phenomena. CAPE is directly connected to the vertical temperature and humidity profiles of the atmosphere, and therefore its temporal and spatial variability can be influenced by temperature and humidity changes near the earth's surface and/or in the upper atmosphere. A global climatology of CAPE has been presented by Riemann-Campe et al. (2009) in terms of seasonal means, variances and trends based on 6-hourly ERA-40 reanalysis data for the 44 yr period 1958–2001. According to Riemann-Campe et al. (2009), CAPE is highest in the tropics with its maxima located over the continents, the seasonal variation is dominated by specific humidity, and the trends for the above period are generally positive for all seasons. For the Mediterranean region, the examination of the climatic characteristics of static stability is an interesting research subject, because of the complicated topography, strong seasonal cycles of most of the climatic parameters, high frequency of extreme weather events, and ongoing climate change affecting the region. Lolis (2007) and Lolis et al. (2012) examined the climate characteristics of atmospheric instability in the Mediterranean region in terms of *K*-index variability, and revealed some in-

*Corresponding author: chlolis@uoi.gr

teresting features, mainly regarding the seasonal variation and spatial distribution of the *K*-index. However, the examination of atmospheric instability in terms of CAPE at a denser grid would provide new useful evidence about the climatology of atmospheric stability over the region, taking into account that the energy available for convection is closely connected to the severity of extreme weather events (e.g. Marsh et al. 2009, Tochimoto & Niino 2017). The connection between CAPE and extreme precipitation in the Mediterranean region is an interesting research subject, and it has been recently examined from various points of view. For example, Ricard et al. (2012) found that long lasting extreme precipitation events over the mountainous Mediterranean area are associated with high CAPE values, Khodayar et al. (2016) detected an increase of CAPE in the hours prior to heavy precipitation events in the Western Mediterranean region, and Rysman et al. (2016) found that the displacement of extreme rain events in the Alps–Mediterranean Euroregion from land to sea from late spring to winter is controlled by CAPE. It is noted that high values of CAPE do not always lead to strong convection, which depends also on convective inhibition (CIN), a parameter that expresses the amount of energy that prevents an air parcel from rising from the surface to the free convection level. However, a detailed description of the climate characteristics of CAPE in the Mediterranean region has the potential to provide useful information regarding the spatial and temporal regimes of static stability, and the vertical profiles of temperature and humidity. In the present study, the climatic characteristics of CAPE over the Mediterranean region are examined using a multivariate statistical approach. The study deals with CAPE, which is an atmospheric stability index significantly affected by the temperature and humidity characteristics of the earth's surface. This is not the case for other stability indices, as for example *K*-index, which has been examined by Lolis (2007) and Lolis et al. (2012), and involves air temperature and humidity not very close to the earth's surface (specifically between the 850 and 500 hPa isobaric levels). Furthermore, the study involves the recently introduced ERA-Interim data set at relatively high resolution (1° × 1°), which reveals relatively small-scale spatial variations associated with the complicated relief of the Mediterranean region that may be hidden when lower resolution data are used (e.g. 2.5° × 2.5°). The main aims of the study are: (1) the identification of the main modes of the seasonal variability of CAPE in the various Mediterranean sub-regions, (2) the identification of the dominant CAPE patterns and the seasons of their predominance, and (3) the detection of the sub-regions of the Mediterranean characterized by statistically significant positive or negative CAPE trends during the last decades. The first 2 aims relate to the main climate characteristics of CAPE over the examined period, while the third one may shed light on ongoing climate change, which is expected to have severe effects in the future over the Mediterranean region (e.g. Adloff et al. 2015).

2. DATA AND METHODOLOGY

The data used are daily (12:00 h UTC) 1° × 1° grid point values of CAPE, 1000 hPa air temperature (T), 1000 hPa specific humidity (Q), 1000 hPa relative humidity (RH), 1000–500 hPa thickness (TH) and 500 hPa air temperature (T_{500}) over the Mediterranean region (10° W to 40° E, 30° to 50° N) (Fig. 1) for the 37 yr period 1979–2015, obtained from the ERA-Interim data base. ERA-Interim is a global atmospheric reanalysis data set produced by the European Centre for Medium-range Weather Forecasts (ECMWF). The ERA-Interim project mainly focused on various difficulties that appeared in the production of ERA-40 reanalysis, related to the hydrological cycle, the stratospheric circulation and the consistency in time of the reanalyzed fields (Dee et al. 2011). CAPE can be defined as:

$$\mathrm{CAPE} = \int_{p_n}^{p_f} (\alpha_p - \alpha_e)\, \mathrm{d}p \qquad (1)$$

where α_e is the environmental specific volume, α_p is the specific volume of a parcel moving upward moist-adiabatically from the free convection level, dp is the differential of atmospheric pressure, p_f is the pressure at the free convection level and p_n is the pressure at the neutral buoyancy level. The unit of measurement of CAPE is J kg^{-1} (AMS 2017).

From the initial daily values of CAPE, the 1979–2015 long-term means for the 73 (73 = 365/5) 5-d periods of the year (averages of all the daily values belonging to each of the 73 5-d periods of the year) are calculated for each of the 1071 grid points of the study area and a 73 × 1071 matrix is constructed. The 1071 columns of the matrix correspond to the 1071 grid points and the 73 lines correspond to the 73 five day periods of the year.

Next, the multivariate statistical method factor analysis (FA) is used as a data reduction tool. FA expresses the p variables X_1, X_2, ... X_p of a data set in terms of a smaller number m of new uncorrelated variables F_1, F_2 … F_m, called the 'factors'. Each of the original variables can be expressed as a linear function of the m factors, i.e.

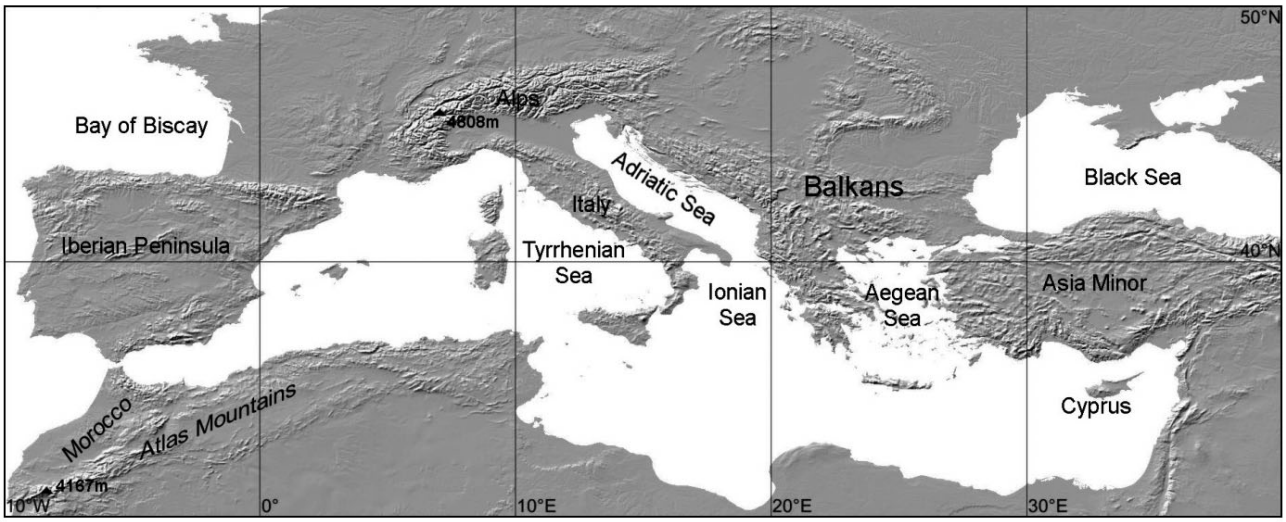

Fig. 1. Study region, indicating the main geographical features mentioned in the text

$$X_i = a_{i1}F_1 + a_{i2}F_2 + \ldots + a_{im}F_m + e_i \quad (2)$$

where the coefficients a_{i1}, a_{i2}, ... a_{im} are the correlation coefficients between the initial variables and the factors, called 'factor loadings' and e_i expresses the part of the variance of X_i which is not explained by the m factors, called 'specificity'. The values of the factors are usually presented in standardized format and they are called 'factor scores' (Jolliffe 1986). FA is a statistical method that presents many similarities to principal component analysis (PCA) (also called empirical orthogonal function [EOF] analysis), which is also used in atmospheric and geophysical research (e.g. Zveryaev & Hannachi 2012, Serra et al. 2014). In fact, PCA is one of the methods used for the extraction of the m factors from the original data set, and this approach is used in the present work. In this case, the factor loadings and the factor scores are obtained with the transformation of the first m principal components using the eigenvectors and the eigenvalues of the correlation matrix of the initial variables (Manly 1986). FA has been applied many times in climatological studies, achieving the appropriate dimensionality reduction and leading to physically interpretable results (e.g. Bartzokas & Metaxas 1995, Jury et al. 2007, Lee et al. 2009). A critical step during the application of FA is the selection of the number of factors m. The decision about this selection can be made with the use of one of the various statistical tests constructed for this purpose (e.g. Overland & Preisendorfer 1982). In the present work, the scree plot method is used for this decision. Specifically, the number of the retained factors has to be equal to the number of the points deviating from the straight line in the scree plot, which is a diagram presenting the eigenvalues of the correlation matrix of the original variables, ordered from highest to lowest (Cattell 1952). The number of factors indicated by the scree plot has been found to be equal or very close to the optimum number of modes explaining the most significant characteristics of the variation of a specific climatic parameter, and at the same time expressing a large percentage of the total variance (e.g. Lolis & Türkeş 2016). There are various modes of FA. In each mode, the lines and the columns of the data matrix correspond to specific physical quantities (e.g. time or space). In the present work S-Mode and T-Mode FA are used. In S-Mode the rows of the matrix correspond to time and the columns correspond to space, while in T-mode the rows and the columns correspond to space and time respectively. S-Mode is applied on the above mentioned 73 × 1071 matrix in order to reveal the main types of mean intra-annual variation of CAPE and the sub-regions of their predominance, while T-Mode is applied on the transposed 1071 × 73 matrix in order to reveal the main types of spatial distribution of CAPE, and the seasons of their prevalence. For S-Mode the factor loadings and the factor scores correspond to space and time respectively, while the reverse is the case for T-Mode, where the loadings and the scores correspond to time and space respectively. Specifically, in S-Mode the scores show the main modes of intra-annual variation of CAPE and the loadings show the areas that correspond to these modes, while in T-Mode the scores show the main modes of spatial distribution of CAPE and the loadings show the seasons of their prevalence. Thus, a comparison between the S-Mode and T-Mode results can only be made by taking into account that

S-Mode refers to the intra-annual variation, while T-Mode refers to the spatial distribution of CAPE. It is noted for example that a maximum (or minimum) found in S-Mode for the intra-annual variation of CAPE over a specific region does not necessarily mean that the results of T-Mode should show a spatial maximum (or minimum) of CAPE over the same region during the same season. This means that CAPE over a specific region can be maximum for example in summer relatively to the other seasons, while at the same time (in summer) it can be minimum relatively to the neighboring regions. Also, the varimax type of orthogonal rotation is performed during the application of FA in order to obtain better discrimination among the initial variables, by maximizing the factor loadings and keeping the factors uncorrelated (Richman 1986).

The rest of the meteorological parameters (T, Q, RH, TH and T_{500}) are used for the interpretation of the intra-annual variations and the patterns of CAPE, which are revealed by S-Mode and T-Mode FA, respectively. The lower troposphere mean lapse rate (LR) is extracted from T, T_{500} and TH [LR = (T – T_{500})/TH] and then parameters T, Q, RH and LR are selected as the potential predictors of CAPE, because they contain basic information about temperature and humidity, especially near the surface. The statistical method stepwise linear regression analysis (SLRA) is applied on the intra-annual variations and patterns of CAPE, T, Q, RH and LR. CAPE is considered as the dependent variable and T, Q, RH and LR are considered as the independent variables. SLRA is a statistical method which predicts a specific variable A by using a set of potential predictor variables B_1, B_2, … B_n. The selection of the appropriate B variables which contribute significantly to the prediction of A is carried out in steps. In each step, a B variable is considered for addition to or subtraction from the set of predictor variables based on a prespecified criterion, which in the present work involves the 0.05 and 0.10 p-values of F to enter and remove a variable, respectively (Draper & Smith 1981). It has to be noted that the potential predictors B_1, B_2, … B_n. do not necessarily need to be uncorrelated, and the absence of a B variable from the final predictors list does not necessarily mean that it is not significantly correlated with variable A. During the SLRA procedure, the addition of a B variable to the predictors list is made when it contributes statistically significantly to the improvement of the prediction of A. A similar approach, i.e. the construction of a linear multi-regression stepwise model for the prediction of a meteorological variable using a list of potential predictors, has been followed by Ziv et al. (2009), who examined the factors controlling lightning activity over Israel. Finally, the Mann-Kendall statistical test is applied on the inter-annual variations of CAPE at each grid point in order to detect the statistically significant positive or negative linear trends during the examined period (WMO 1966, Kendall 1975).

3. RESULTS AND DISCUSSION

In the following subsections, the results regarding the seasonal variability (Section 3.1), the spatial distribution (3.2) and the trends of CAPE (3.3) are presented and discussed.

3.1. Seasonal variability

The application of S-Mode FA on the 73 × 1071 data matrix reveals 4 main modes of CAPE intra-

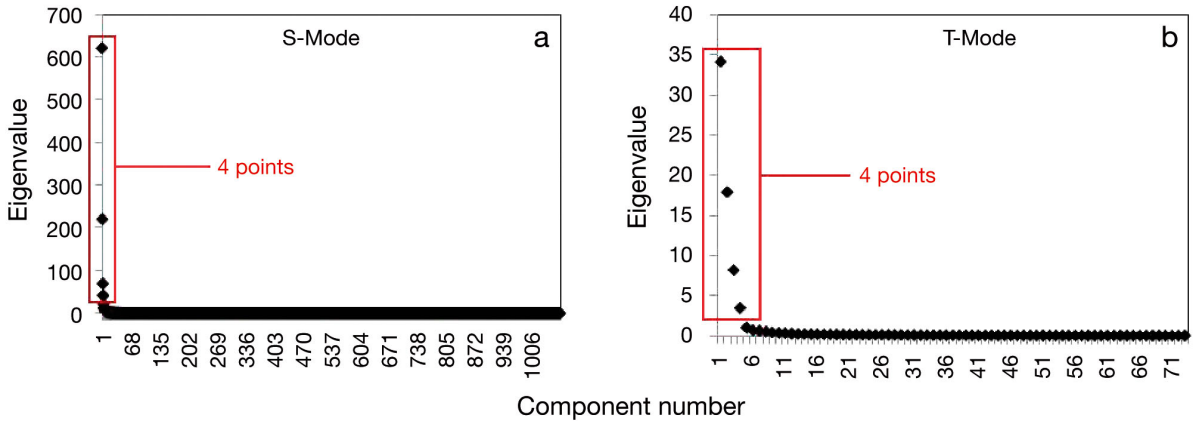

Fig. 2. Scree plots for factor analysis of (a) the intra-annual variation (S-Mode) and (b) the spatial distribution (T-Mode) of convective available potential energy (CAPE) in the Mediterranean region

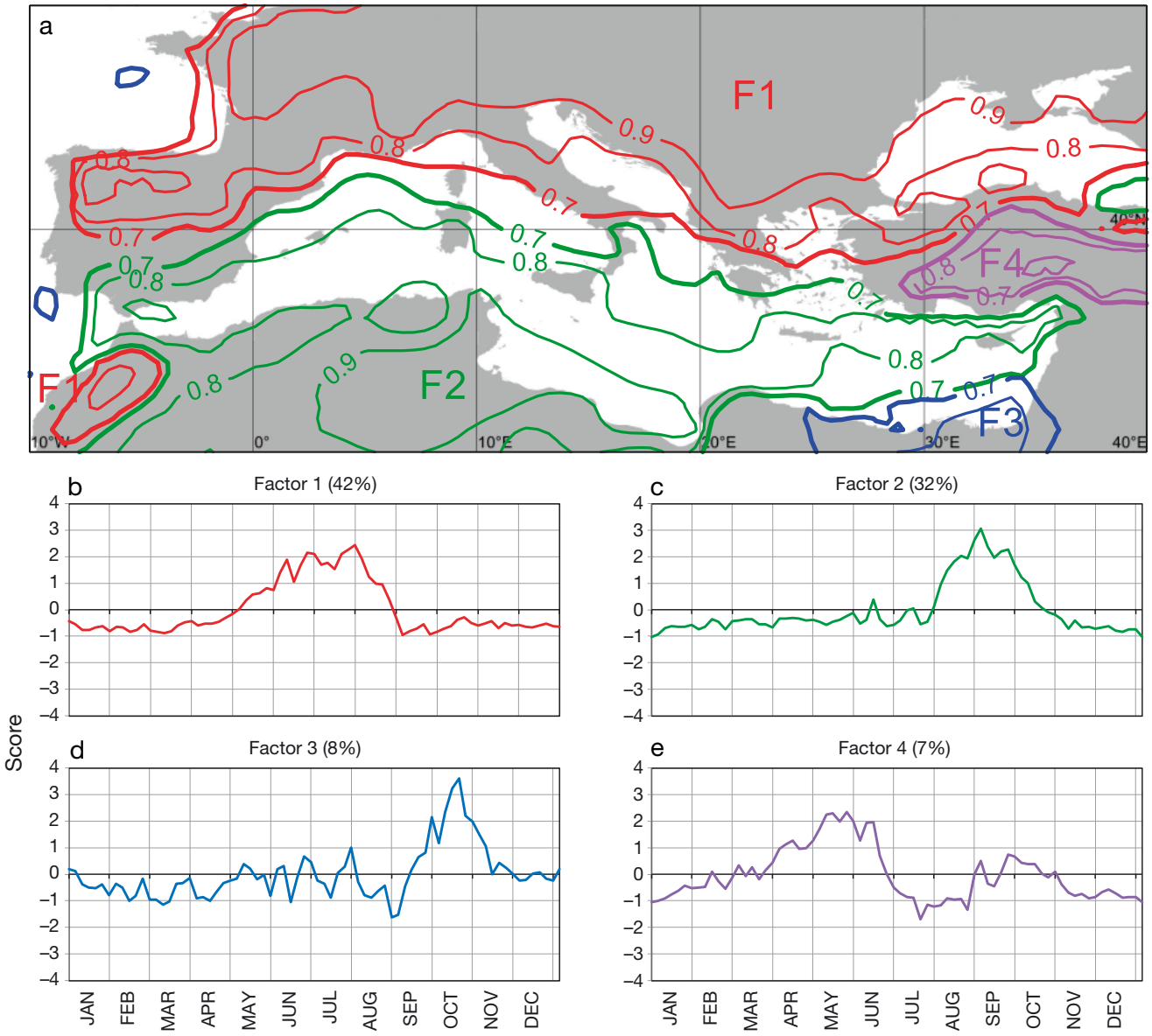

Fig. 3. S-Mode factor analysis: (a) the spatial distribution of loadings (isopleths for loadings ≥0.7 are shown); (b–e) the intra-annual variations of factor scores (standardized values)

annual variation accounting for 89 % of the total variance. The scree plot is presented in Fig. 2a. The spatial distribution of loadings is presented in Fig. 3a, which shows the sub-regions that correspond to each of the 4 modes. The intra-annual variations of scores are presented in Figs. 3b–e, and they are in fact the corresponding intra-annual variations of CAPE over the above sub-regions in standardized format. For each factor, SLRA is applied on CAPE, *T*, *Q*, RH and LR intra-annual variations at the grid points with the maximum factor loading. The grid point with the maximum factor loading is selected, because it is characterized by the maximum correlation between the factor scores and CAPE time series. This means that for a grid point with a high factor loading, the intra-annual variations of CAPE and factor scores are almost identical. The results of SLRA are presented in Table 1 and the intra-annual variations of CAPE and the corresponding predictor parameters are shown in Fig. 4. It is noted that the parameters which are not found by SLRA to contribute significantly to the prediction of CAPE are not necessarily uncorrelated with CAPE, and probably a part of their variance overlaps with the variance of the predictors.

Table 1. Stepwise linear regression analysis for S-Mode factor analysis, i.e. the predictors of CAPE and the corresponding R values for the grid points with the highest factor loadings. **Bold**: best model results

Factor	Model	Predictors	R
Seasonal variation of CAPE at:			
(F1) 28° E, 48° N	1	Q	0.850
	2	Q, T	0.880
	3	**Q, T, LR**	**0.963**
(F2) 6° E, 33° N	1	**Q**	**0.864**
(F3) 32° E, 31° N	1	Q	0.324
	2	Q, LR	0.584
	3	**Q, LR, T**	**0.904**
(F4) 35° E, 38° N	1	LR	0.482
	2	LR, RH	0.829
	3	**LR, RH, Q**	**0.886**

The first mode (F1) accounts for 42% of the total variance, and corresponds to the area of central Europe, the northern Mediterranean coasts and the Black Sea (Fig. 3a). It is characterized by a maximum in summer, specifically during June and July (Fig. 3b). According to the results of SLRA (Table 1), the main CAPE predictors are *Q*, *T* and LR (R = 0.963). According to Fig. 4a, the maximum of the CAPE intra-annual variation coincides with the corresponding maxima of *T* and *Q*. LR is also high in summer, although its maximum appears a little earlier (late spring). The high LR over central Europe in summer is associated with the intense land heating and the presence of relatively colder upper air masses. During the cold period of the year, CAPE is lower, because the land cooling and the frequent presence of anticyclonic conditions reduce the prevailing lapse rate in the lower troposphere (Lolis et al. 2012).

The second mode (F2) accounts for 32% of the total variance and corresponds to the southern Mediterranean Sea and a part of NW Africa (Fig. 3a). According to the seasonal variation of scores (Fig. 3c), CAPE is maximum between late summer and early autumn. This late summer to early autumn maximum can be attributed to the high air temperature and humidity of the lowest tropospheric layers associated with the high sea surface temperature (SST) of the southern Mediterranean Sea, and the intense land warming over NW Africa and considerably lower air temperatures over the middle troposphere, taking into account that in early autumn the subtropical zone has started moving southwards and the first cold air masses prevail in the middle troposphere, increasing static instability. The application of SLRA indicates that *Q* is the main predictor of CAPE (R = 0.864) (Table 1, Fig. 4b), providing a significant evidence regarding its dominant role in the seasonal variation of static stability over the specific region.

The third mode (F3) accounts for 8% of the total variance and prevails over a small region comprising the northern Egyptian coasts (Fig. 3a). The intra-

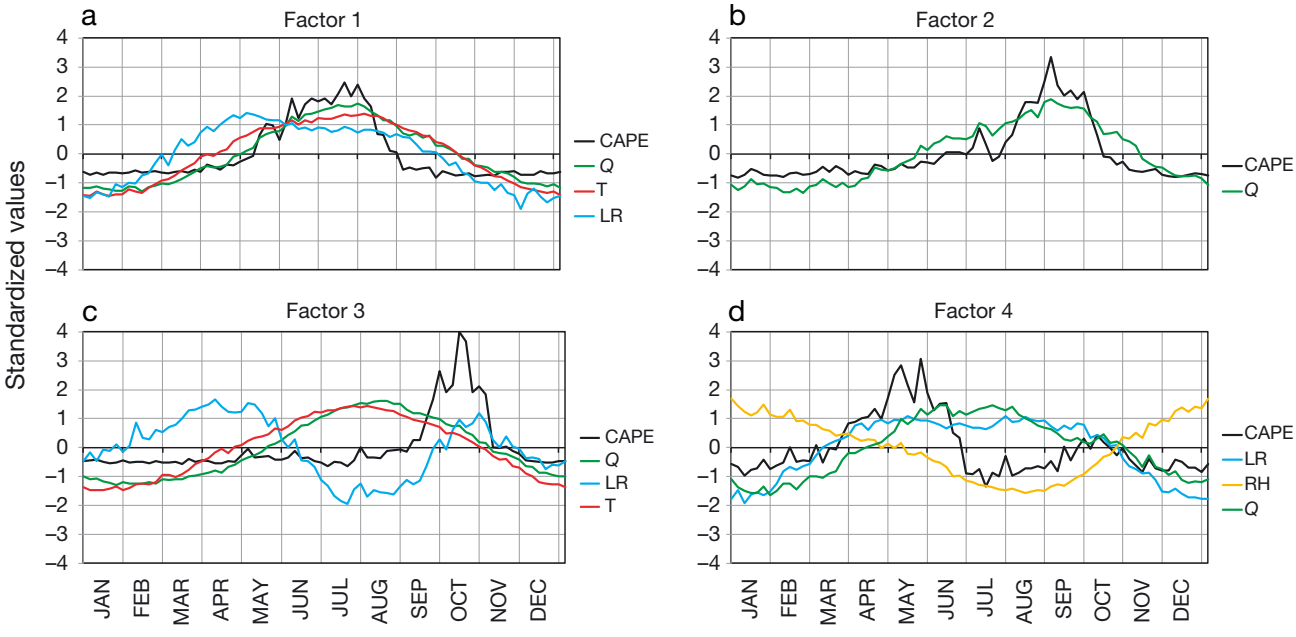

Fig. 4. The intra-annual variations of CAPE and its predictors 1000 hPa air temperature (*T*), 1000 hPa specific humidity (*Q*), 1000 hPa relative humidity (RH) and lower troposphere mean lapse rate (LR) (standardized values), for the grid points with the highest loadings for (a–d) factors 1–4, respectively

annual variation of scores shows a maximum in October, about 1.5 mo later than in the case of F2 (Fig. 3d). This time lag is possibly due to the gradual southwards displacement of the subtropical zone and the corresponding prevalence of the westerly circulation, which delays slightly over the eastern part of the southern Mediterranean. According to the SLRA results (Table 1, Fig. 4c), the predictors of CAPE seasonal variation over this area are *T*, *Q* and LR. The October CAPE maximum can be explained by taking into account the corresponding October maximum of LR, and the fact that in October both *T* and *Q* are relatively high. During the rest of the year CAPE is lower, because high LR generally coincides with low *T* and *Q* and vice versa.

Finally, the fourth mode (F4) accounts for 7% of the total variance, and corresponds to the continental region of Asia Minor (Fig. 3a). It is characterized by maxima in May and in early autumn, and minima in high summer months (July and August) and in winter (Fig, 3e). The above 2 maxima are in agreement with those revealed by Lolis & Türkeş (2016) in the intra-annual variation of the extreme precipitation days in Turkey, regarding the only warm period cluster found associated with high CAPE values over this region. The maxima of late spring and early autumn can be attributed to the high surface temperature associated with the intense land warming, along with the presence of significantly colder upper air masses. The July–August minimum, which splits the high static instability maximum of the warm period into the above 2 maxima, is probably caused by of the low relative humidity near the earth's surface, along with the mid-level subsidence associated with the Asian monsoon (Ziv et al. 2004, Rizou et al. 2015). The significant role of RH in the summer minimum of CAPE over this region is shown in the SLRA results (Table 1, Fig. 4d). RH is one of the predictors, and its summer minimum is responsible for the presence of 2 maxima (spring and autumn) in the seasonal variation of CAPE, instead of 1 broad maximum in summer, which would be the result of the corresponding maxima in the *Q* and LR seasonal variations.

3.2. Spatial variability

The application of T-Mode FA on the transposed 1071 × 73 matrix reveals 4 dominant patterns of CAPE in the Mediterranean region, accounting for 87% of the total variance. The scree plot is presented in Fig. 2b. The intra-annual variation of loadings and the spatial distributions of scores are presented in Fig. 5. The intra-annual variations of loadings show the seasons of the predominance of the 4 patterns, and the patterns of the scores show the spatial distribution (standardized) of CAPE during these seasons. It appears that the 4 modes generally correspond to the 4 conventional seasons of the year. This means that in the case of the spatial distribution of CAPE, the alteration among the dominant patterns coincides with the alteration among the conventional seasons. This is not the case for other parameters over the same region (e.g. atmospheric circulation) (Lolis et al. 2008). Similarly to Section 3.1, for each factor, SLRA is applied on CAPE, *T*, *Q*, RH and LR patterns for the months with the maximum factor loadings (maximum of the monthly averages). The month with the maximum factor loadings is selected, because it is characterized by the maximum correlation between the factor scores and CAPE patterns. This means that for the month with the highest factor loadings, CAPE and factor score patterns are almost identical. The results of SLRA are presented in Table 2, and the patterns of the 2 most significant (according to SLRA) predictor parameters for each case are shown in Figs. 6–9 below.

The first mode (F1) accounting for 24% of the total variance prevails in autumn (loadings above 0.7) (Fig. 5b), and the associated pattern is characterized by high values over the Mediterranean Sea and especially over its southern part, and low values mainly over the northern continental areas (Fig. 5a). This spatial distribution is in agreement with the fact that in autumn the sea surface is warm relative to the overlying air, which becomes colder because of the first cold air masses affecting the Mediterranean after the beginning of the cold and rainy period of the year. The relatively high LR and *Q* values over the lower tropospheric layers are responsible for the CAPE maxima over the sea, which are in agreement with the spatial distribution of lightning activity during this season (Galanaki et al. 2015, Kotroni & Lagouvardos 2016). According to the SLRA results (Table 2, Fig. 6), the CAPE predictors for the month with the highest F1 loadings (October) are all the associated parameters *Q*, LR, *T* and RH (R = 0.876). *Q* appears as the main predictor, giving a high value of R (R = 0.811) and the addition of the rest of the parameters does not greatly increase this value. In the patterns of the first 2 predictors (*Q* and LR), it can be seen that there is a similarity between *Q* and the factor 1 score patterns (CAPE in October), while the high LR over North Africa cannot contribute to high CAPE values there, because of the very low *Q* over the same area.

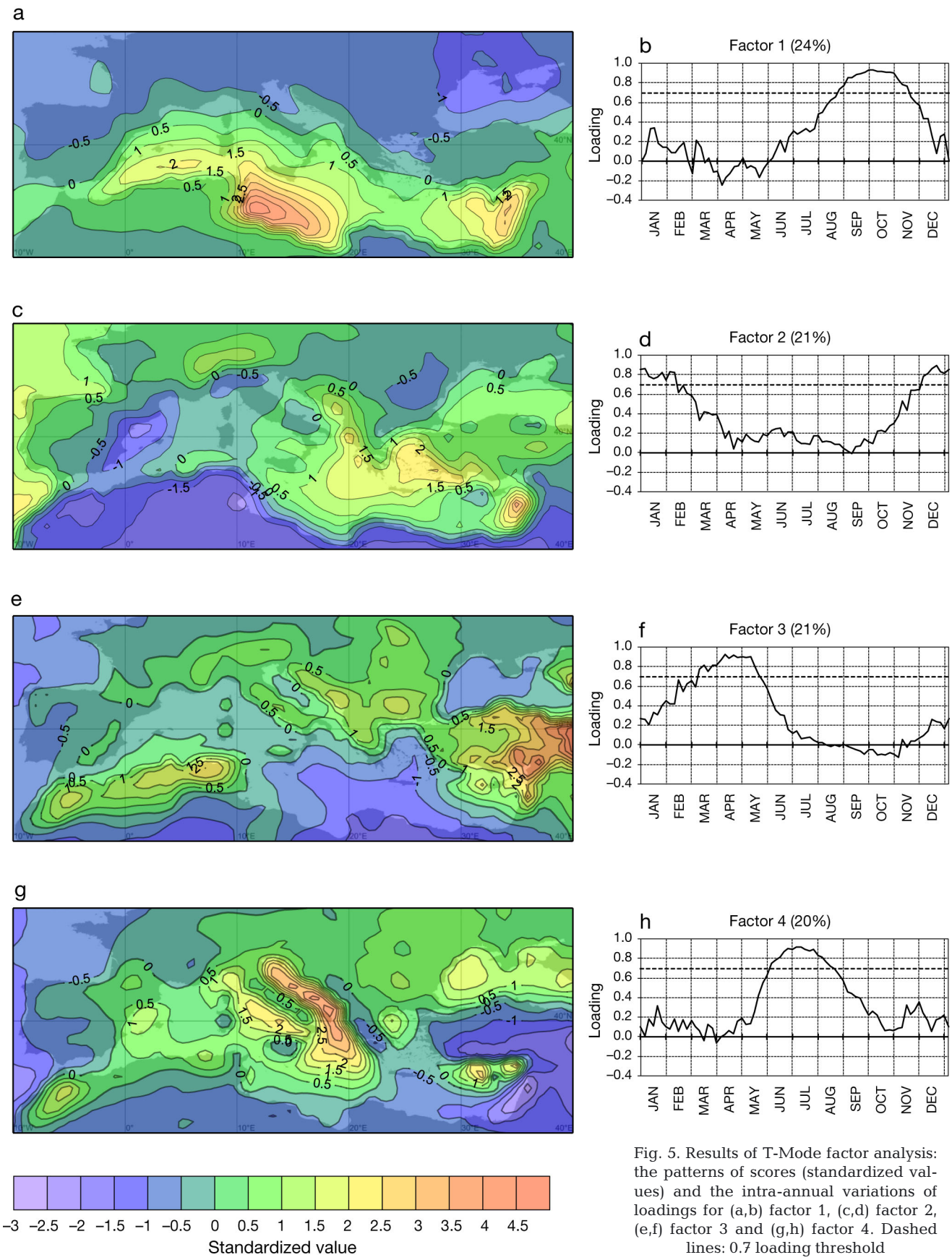

Fig. 5. Results of T-Mode factor analysis: the patterns of scores (standardized values) and the intra-annual variations of loadings for (a,b) factor 1, (c,d) factor 2, (e,f) factor 3 and (g,h) factor 4. Dashed lines: 0.7 loading threshold

Table 2. Stepwise linear regression analysis for T-Mode factor analysis, i.e. the predictors of CAPE patterns and the corresponding R values for the months with the highest factor loadings. **Bold**: best model results

Factor	Model	Predictors	R
CAPE pattern			
(F1) October	1	Q	0.811
	2	Q, LR	0.840
	3	Q, LR, T	0.875
	4	**Q, LR, T, RH**	**0.876**
(F2) December	1	RH	0.505
	2	RH, LR	0.813
	3	RH, LR, T	0.815
	4	**RH, LR, T, Q**	**0.820**
(F3) April	1	LR	0.223
	2	LR, RH	0.813
	3	LR, RH, T	0.818
	4	**LR, RH, T, Q**	**0.819**
(F4) July	1	Q	0.590
	2	Q, LR	0.682
	3	Q, LR, T	0.767
	4	**Q, LR, T, RH**	**0.778**

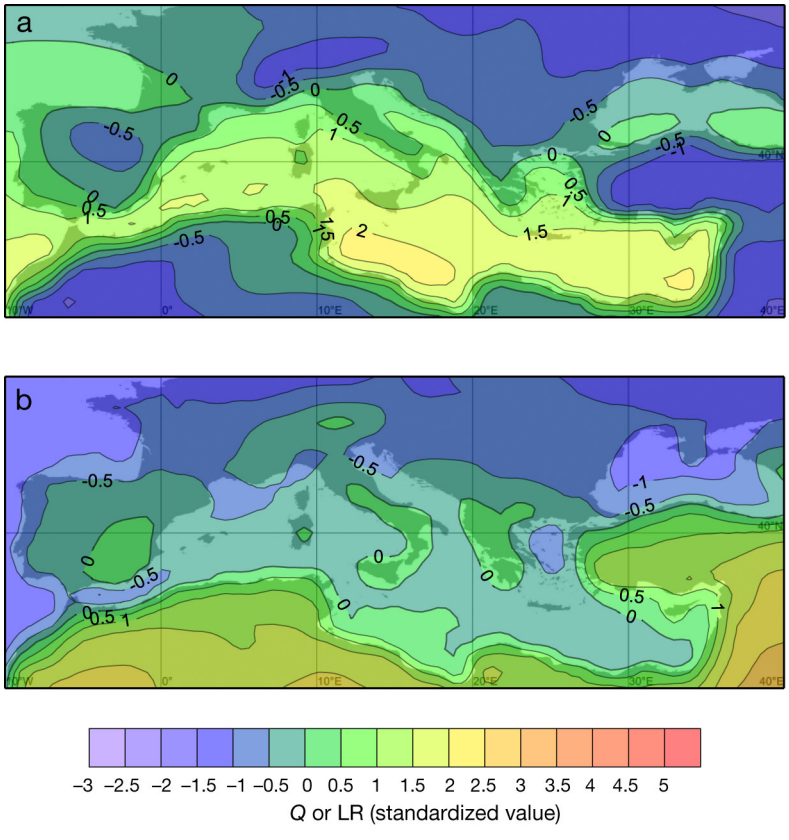

Fig. 6. The patterns of (a) *Q* and (b) LR (standardized values), the first 2 predictors of CAPE pattern for October. See Fig. 4 legend for abbreviations of predictors

The second mode (F2) accounts for 21% of the total variance and prevails in winter (Fig. 5d). According to the spatial distribution of scores, the highest values appear over the Eastern Mediterranean Sea, while the lowest values are shown over the Northern Africa continental areas (Fig. 5c). This spatial distribution can be attributed to the fact that in winter middle troposphere cyclonicity is maximum over the Eastern Mediterranean Sea leading to high LR values because of the associated cold upper air masses prevailing over the relatively warm sea (e.g. Lolis et al. 2008). The NW Africa minimum is a result of the low humidity near the surface and the action of the subtropical anticyclone. The SLRA results (Table 2, Fig. 7) show that the predictors for the month with the highest F2 loadings (December) are all the associated parameters, but the order is different than in the case of autumn. Specifically the order of the parameters is RH, LR, *T* and *Q* and R = 0.820. RH and LR appear as the main predictors, giving a high R value (R = 0.813), while the addition of the other 2 parameters does not greatly increase this value. In Fig. 7, it is seen that the Eastern Mediterranean maximum of CAPE is mainly attributed to the corresponding maximum of LR over the same area, while the NW Africa CAPE minimum is mainly due to the very low RH values there.

The third mode (F3) accounts for 21% of the total variance, and according to the intra-annual variation of loadings, it prevails in spring (Fig. 5f). The pattern of scores shows that high values of CAPE appear mainly in the continental areas, especially over the Balkans, Asia Minor and the Atlas Mountains (Fig. 5e). In spring, the intense land heating and the persistence of cold air masses in the middle troposphere are generally responsible for high static instability over the continental areas. The static instability is highest over low latitude inland areas (e.g. Asia Minor and Atlas Mountains), because the daytime solar radiation is higher there, contributing to more intense land heating and higher low level lapse rates. The high CAPE over the Atlas Mountains is in agreement with the prevailing synoptic conditions over this area in spring. These conditions are associated with the initiation of the Saharan depressions (Prezer-

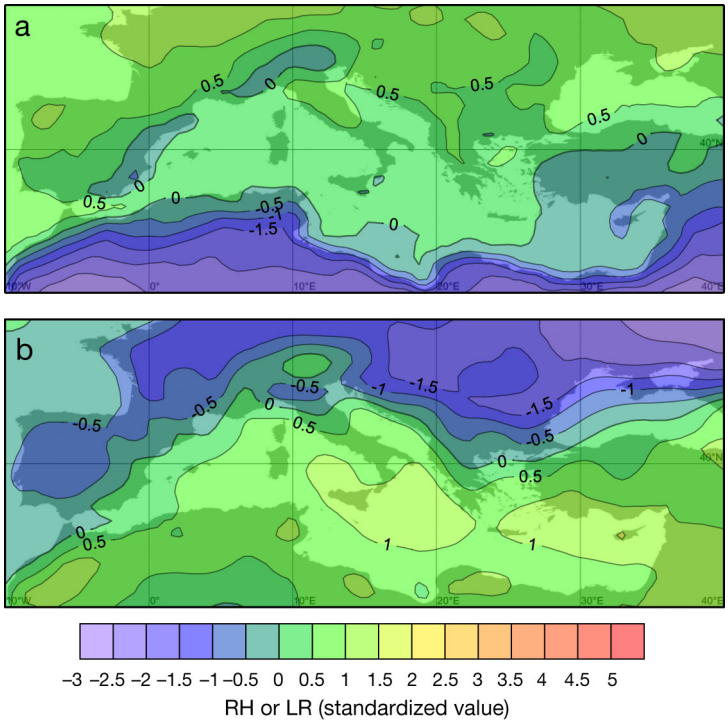

Fig. 7. The patterns of (a) RH and (b) LR (see Fig. 4 legend for description) (standardized values), the first 2 predictors of CAPE pattern for December

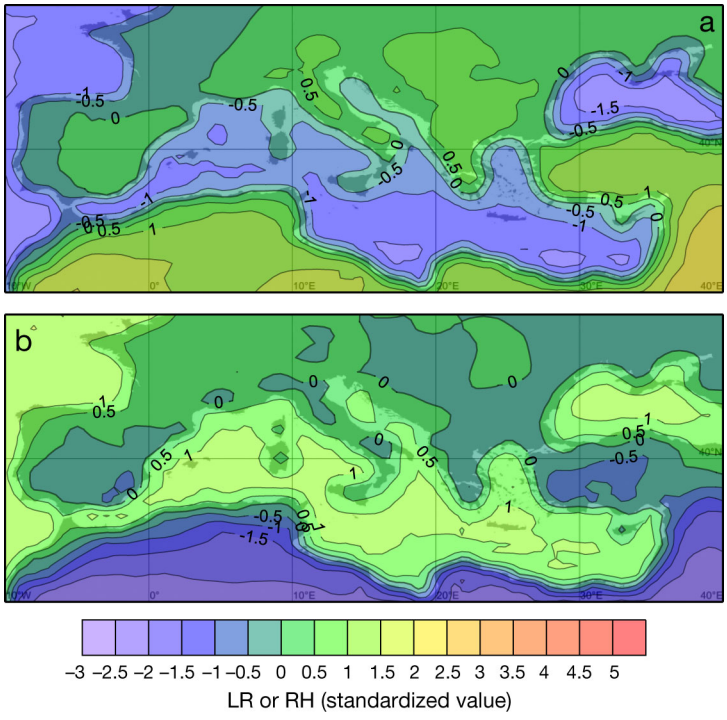

Fig. 8. The patterns of (a) LR and (b) RH (standardized values), the first 2 predictors of CAPE pattern for April. See Fig. 4 legend for abbreviations of predictors

akos et al. 1990). According to the SLRA results (Table 2, Fig. 8), for the month with the highest F3 loadings (April) all the parameters contribute to the prediction of CAPE and the order is LR, RH, *T* and *Q* (R = 0.819). LR and RH are the main predictors, giving a relatively high R (R = 0.813) and the addition of the rest of the parameters does not greatly increase this value. In Fig. 8, it can be seen that the LR maximum over Turkey and the Middle East is responsible for the high CAPE values there, while the gradual decrease of RH towards the interior of Africa allows the prevalence of static instability conditions only near the coast and specifically along the Atlas Mountain Range.

The fourth mode (F4) (20% of the total variance) prevails in summer (Fig. 5h) and the pattern of scores reveals CAPE maxima over the marine areas of the Adriatic Sea, the Tyrrhenian Sea, the Cyprus region and the Black Sea (Fig. 5g). This result seems strange at first, as it might be expected that CAPE maxima would be located over the continental areas because of the intense land heating and not over the relatively cold sea surface. However, in summer, the presence of cold upper air masses is not so frequent, and the spatial distribution of CAPE is mainly controlled by the corresponding spatial distribution of specific humidity near the surface (Riemann-Campe et al. 2009). *Q* is high over the sea surface in summer, and it is the main factor that contributes to the high CAPE values over the sea areas. The strong maxima over the Adriatic and Ionian Seas and the Cyprus region can also be attributed to the fact that over these areas (1) the middle troposphere is colder relative to the Western Mediterranean Sea where the subtropical anticyclone dominates and (2) the northerly flow is weak relative to e.g. the Aegean Sea area, where the etesian winds dominate (Anagnostopoulou et al. 2014, Dafka et al. 2016), reducing air temperature near the surface and increasing static stability. The application of SLRA reveals that that for the month with the highest F4 loadings (July), all the associated parameters contribute to the prediction of CAPE and the order is *Q*, LR, *T* and RH (R = 0.778), as was the case for autumn (Table 2, Fig. 9). According to the patterns of the factor 4 scores and

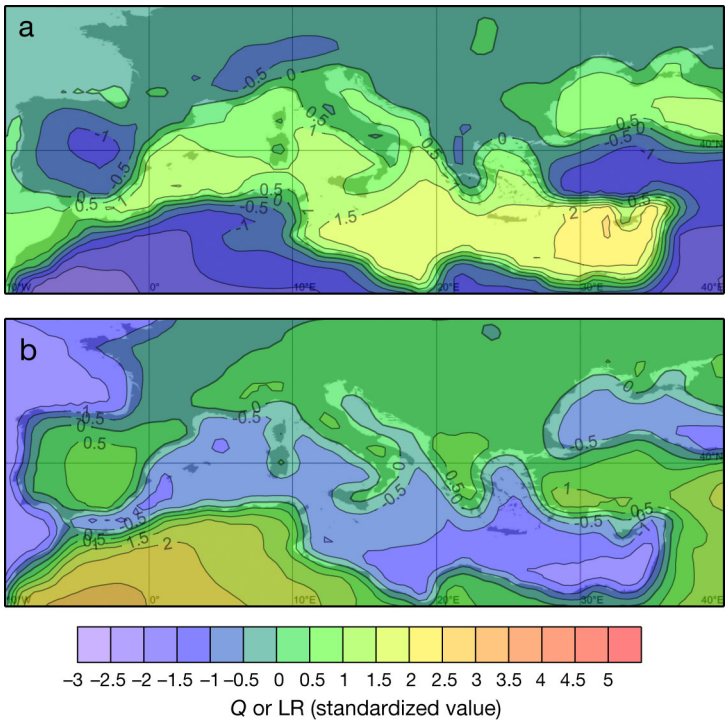

Fig. 9. The patterns of (a) *Q* and (b) LR (standardized values), the first 2 predictors of CAPE pattern for July. See Fig. 4 legend for abbreviations of predictors

the most significant predictors (*Q* and LR), the maxima and minima of CAPE appear over areas with high and low *Q* respectively. More specifically, the maximum over the Adriatic Sea is also favored by the relatively high LR (higher than the other sea areas with lower latitudes) (Fig. 9).

3.3. Trends

The linear trends of the inter-annual variations of the monthly values of CAPE are calculated for the 12 months and for 1979–2015, and the Mann-Kendall statistical test is used in order to reveal the statistical significant trends at the 95% confidence level. According to Fig. 10, the magnitude of trends is higher during the warm period of the year when the mean values of CAPE and the static instability in general are higher relative to the cold period. In January, statistically significant positive trends are found over a small area of central Europe and over a part of the Eastern Mediterranean Sea including the Aegean Sea, while there are almost no statistically significant negative trends. In February, positive trends are found over the Aegean Sea, over a part of the Ionian Sea and Albania, and north of the Black Sea, while significant negative trends are found mainly over the NE African coast. In March, the areas of significant positive trends include the SW Balkans, the Ionian Sea, West Asia Minor and the Eastern Black Sea, while significant negative trends appear over central Europe, the NE African coast and the Middle East. In April and in May the area of significant positive trends is larger, comprising principally a large part of the Central and the Eastern Mediterranean and the western Black Sea, while significant negative trends are found in April over the Middle East. In summer months, a large part of the Central and the Eastern Mediterranean region and the Black Sea are characterized by significant positive trends, while significant negative trends are found only over a part of the Iberian Peninsula and Morocco. In September the positive trend area remains almost the same as in August, while significant negative trends are confined over Morocco. In October, the area of the significant positive trends covers mainly the SE Balkans, the Aegean and a part of the Black Sea, while there are almost no significant negative trends. In November, significant positive trends are found over the Bay of Biscay, the areas of Sardinia and southern Italy and the Eastern Mediterranean south of Cyprus, while in December significant positive trends are found over the Aegean and the Ionian Seas.

The positive trends found especially during the warm period of the year over the Central and the Eastern Mediterranean region can be partly connected to ongoing climate change, providing an indication of the current and future increase in the frequency and intensity of extreme weather events over the region (e.g. Hertig et al. 2014). In order to ascertain the factors that led to increases in CAPE, we used the statistically significant (95% confidence level) linear trends of *T*, *Q*, RH and LR for the regions with positive statistical significant trends in CAPE, and that for the 4 core months defined in the previous section (October, December, April and July). These statistically significant linear trends, as well as the corresponding inter-annual variations, are presented, along with the CAPE variations in Fig. 11. For October, a statistically significant positive trend is found for *Q* only (Fig. 11a), while for December the only parameter that shows statistically significant increase is *T* (Fig. 11b). For April, both parameters (*T* and *Q*) present significant positive trends (Fig. 11c).

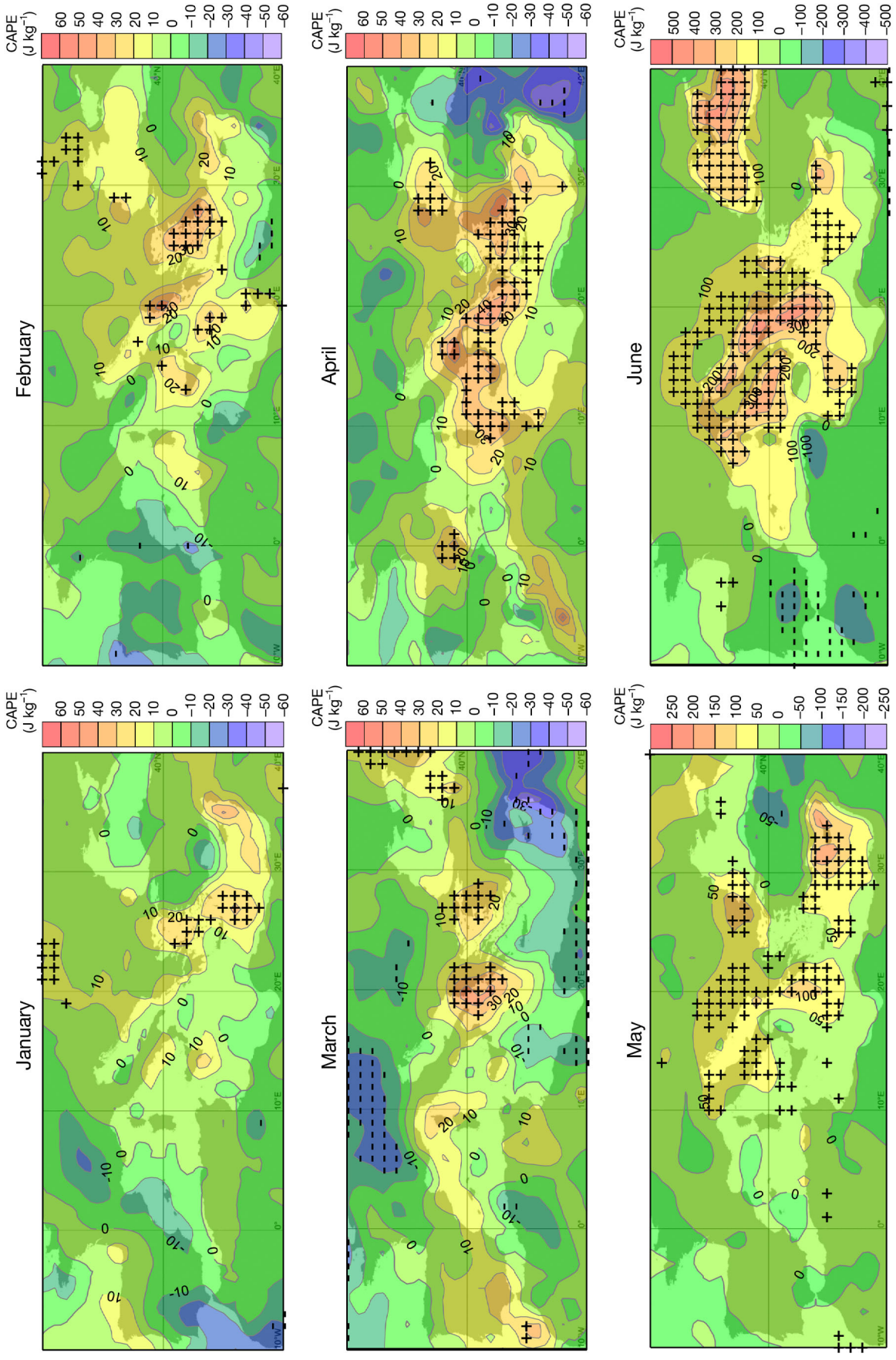

Fig. 10. The monthly patterns of the linear trends of CAPE (J kg^{-1}) for the 37 yr period 1979–2015. Positive and negative statistically significant (95% confidence level) trends are marked using + and – signs, respectively

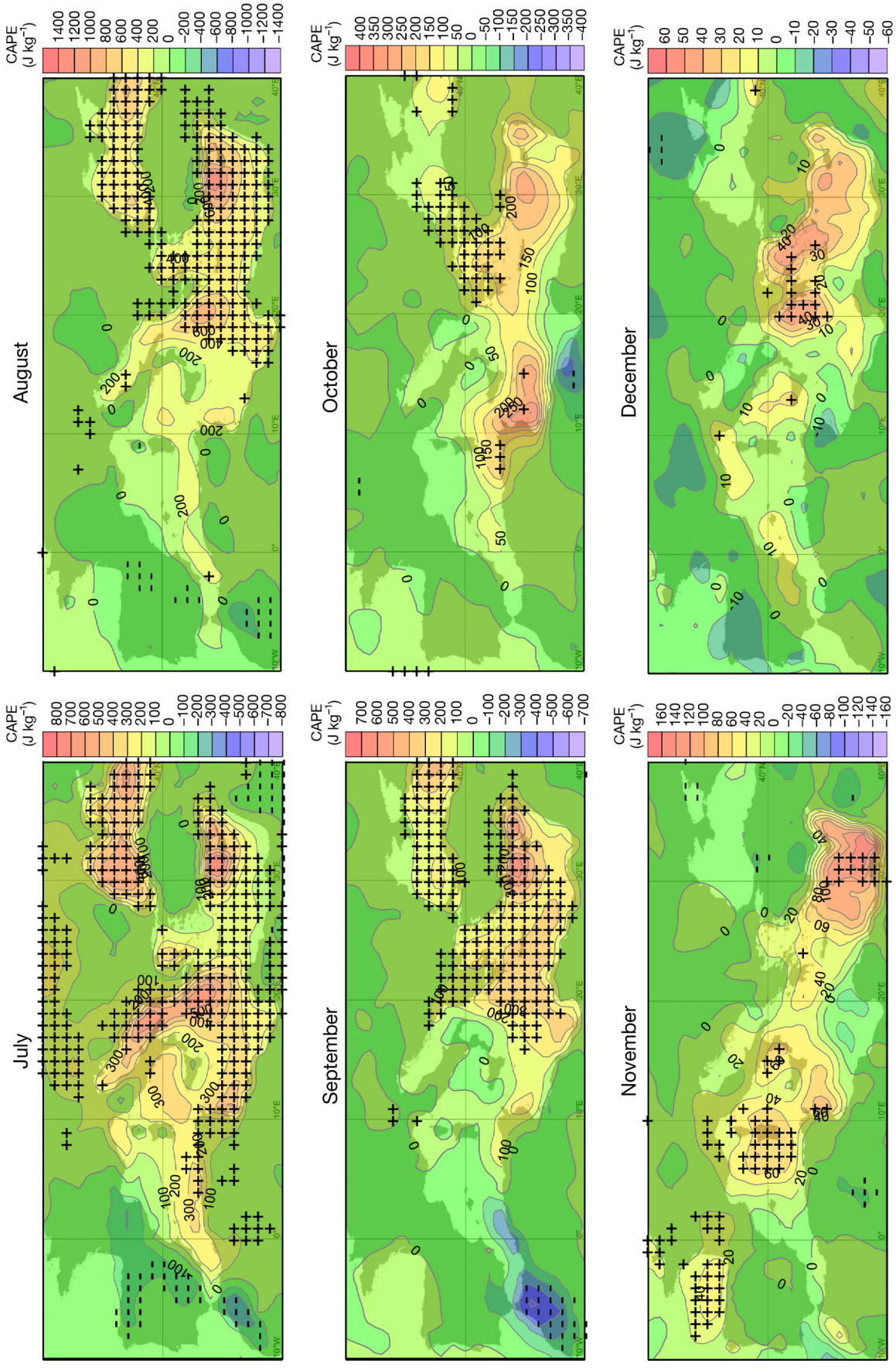

Fig. 10 (continued)

For July, all parameters present significant linear trends (Fig. 11d). Specifically *T*, *Q* and LR are characterized by positive trends, while RH shows a negative trend. The results for July show that the LR increase is one of the main causes for the positive trend of CAPE over a large part of the Mediterranean region. Taking into account that the increase in LR is accompanied by a simultaneous increase in air temperature near the surface, it seems that the surface atmospheric layers are becoming much warmer relative to those of the middle troposphere. This means that in summer, the recent warming is more intense in the lowest atmospheric layers. On the other hand, the reduction in RH can be attributed to the corresponding increase in *T*, a parameter which directly affects RH. In this case, it seems that CAPE is more sensitive to the change in the vertical temperature profile than to the reduction in surface relative humidity.

4. CONCLUSIONS

The main climate characteristics of CAPE in the Mediterranean region for the period 1979–2015 are examined, with the following conclusions:

1. Four main modes of intra-annual variation of CAPE are found. These modes correspond to specific sub-regions of the area under study, and they are mainly associated with variations in circulation, temperature and humidity in the middle and lower troposphere, which modulate atmospheric stability. The influence of the various atmospheric parameters on the seasonal variation of CAPE is different among the Mediterranean sub-regions.

2. Four main modes of spatial distribution of CAPE are found. These modes correspond to the 4 seasons of the year, and each mode is connected to the specific climate characteristics of the corresponding season. These characteristics are determined by dominant global-scale circulation patterns and the temperature and humidity characteristics of the earth's surface (land or sea), which in turn depend mainly on solar radiation levels and the difference in thermal inertia between land and sea. All patterns are significantly related to the lapse rate of the lower troposphere. Furthermore, the winter and spring CAPE patterns are mainly associated with relative humidity near the surface, while summer and autumn patterns are mainly associated with specific humidity near the surface.

3. Statistically significant positive linear trends are found for a large part of the Central and Eastern Mediterranean region, especially in summer. These

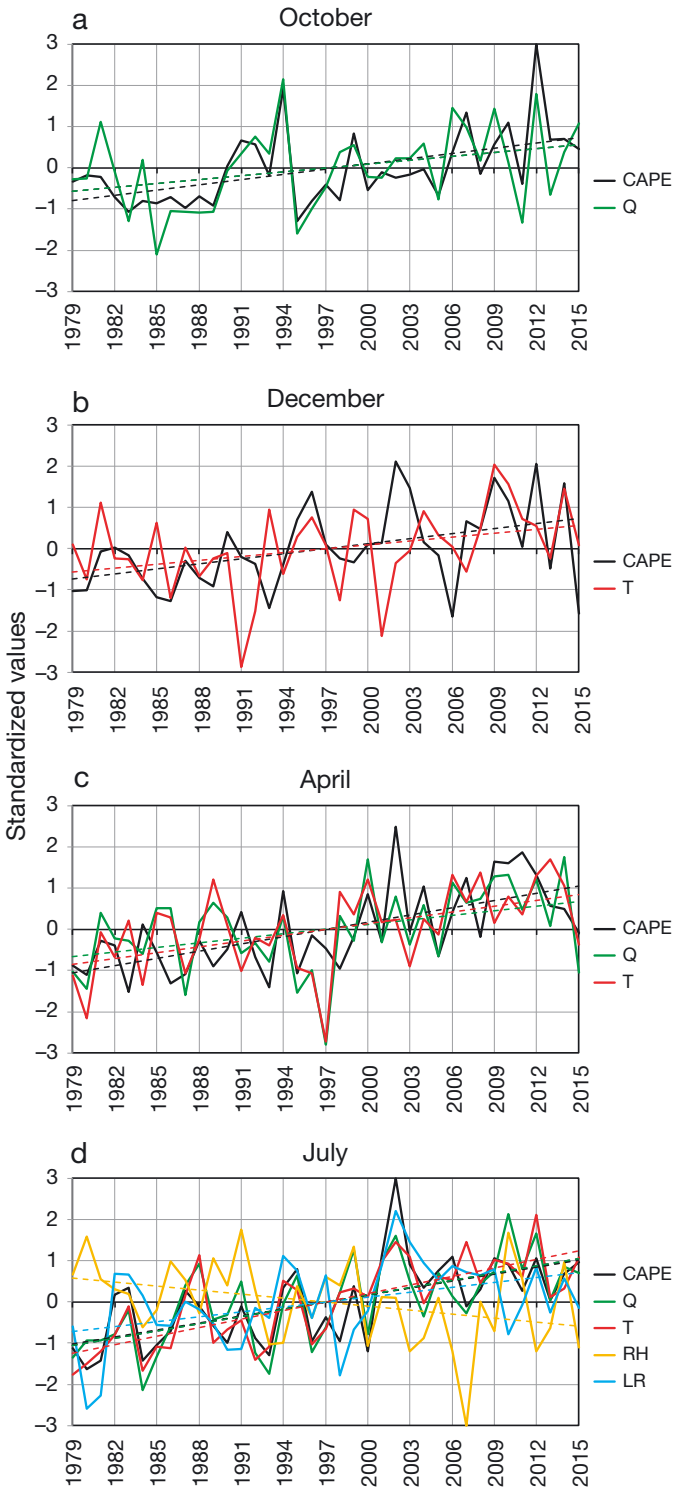

Fig. 11. The inter-annual variations of CAPE and (a) *Q* for October, (b) *T* for December, (c) *Q* and *T* for April and (d) *Q*, *T*, RH and LR for July (standardized values) for the areas characterized by positive CAPE trends. The statistically significant (95% confidence level) trends for each variable are presented with dashed lines. See Fig. 4 legend for abbreviations of meteorological variables

positive trends indicate a significant increase in static instability, which can be attributed to the corresponding temperature and humidity trends near the surface, and the lapse rate.

4. The comparison of the results of the present study with the results of other studies dealing with the seasonal variation and spatial distribution of atmospheric stability and other related parameters over the Mediterranean region provides useful evidence about the similarities or differences among the various stability indices, and the degree of dependence of atmospheric stability climatology on other climatic parameters.

5. The detailed spatial distribution and seasonal variation of static instability trends over the Mediterranean region during recent decades are significant factors that have to be carefully taken into account by the climate researchers, since they can be linked to the vertical profiles of trends of other parameters such as temperature and humidity, possibly revealing a different behavior between the surface and upper atmosphere.

The examination of the connection among the main climatic characteristics of CAPE presented in the present study, the climatic characteristics of other static stability indices, and the corresponding modes of convective precipitation and lightning activity over the same area could be considered as a subject of future research. Such a study could provide useful evidence about the ability of the stability indices to predict convective precipitation and thunderstorms (taking into account that this ability could depend on the season of the year). Finally, a more detailed analysis is needed on the factors responsible for the increase in static instability during recent decades. Such an analysis could comprise a detailed examination of temperature and humidity variability at various atmospheric levels for each season or 10 d period of the year.

LITERATURE CITED

Adloff F, Somot S, Sevault F, Jordà G and others (2015) Mediterranean Sea response to climate change in an ensemble of twenty first century scenarios. Clim Dyn 45: 2775–2802

AMS (American Meteorological Society) (2017) Convective available potential energy. Glossary of meteorology. http://glossary.ametsoc.org/wiki/Convective_available_potential_energy

Anagnostopoulou C, Zanis P, Katragkou E, Tegoulias I, Tolika K (2014) Recent past and future patterns of the Etesian winds based on regional scale climate model simulations. Clim Dyn 42:1819–1836

Bartzokas A, Metaxas DA (1995) Factor Analysis of some climatological elements in Athens, 1931–1992: covariability and climatic change. Theor Appl Climatol 52:195–205

Cattell RB (1952) Factor analysis. Harper, New York, NY

Dafka S, Xoplaki E, Toreti A, Zanis P, Tyrlis E, Zerefos C, Luterbacher J (2016) The Etesians: from observations to reanalysis. Clim Dyn 47:1569–1585

Dee DP, Uppala SM, Simmons AJ, Berrisford P and others (2011) The ERA-Interim reanalysis: configuration and performance of the data assimilation system. QJR Meteorol Soc 137:553–597

Draper N, Smith H (1981) Applied regression analysis, 2nd edn. John Wiley & Sons, New York, NY

Galanaki E, Kotroni V, Lagouvardos K, Argiriou A (2015) A ten-year analysis of cloud-to-ground lightning activity over the Eastern Mediterranean region. Atmos Res 166: 213–222

Hertig E, Seubert S, Paxian A, Vogt G, Paeth H, Jacobeit J (2014) Statistical modelling of extreme precipitation indices for the Mediterranean area under future climate change. Int J Climatol 34:1132–1156

Jolliffe IT (1986) Principal component analysis. Springer, New York, NY

Jury M, Malmgren BA, Winter A (2007) Subregional precipitation climate of the Caribbean and relationships with ENSO and NAO. J Geophys Res Atmos 112:D16107

Kendall MG (1975) Rank correlation methods, 4th edn. Charles Griffin, London

Khodayar S, Kalthoff N, Kottmeier C (2016) Atmospheric conditions associated with heavy precipitation events in comparison to seasonal means in the western Mediterranean region. Clim Dyn, doi:10.1007/s00382-016-3058-y

Kotroni V, Lagouvardos K (2016) Lightning in the Mediterranean and its relation with sea-surface temperature. Environ Res Lett 11:034006

Lee CK, Shen SSP, Bailey B, North GR (2009) Factor analysis for El Niño signals in sea surface temperature and precipitation. Theor Appl Climatol 97:195–203

Lolis CJ (2007) Climatic features of atmospheric stability in the Mediterranean region (1948–2006): spatial modes, inter-monthly and inter-annual variability. Meteorol Appl 14:361–379

Lolis CJ, Türkeş M (2016) Atmospheric circulation characteristics favoring extreme precipitation in Turkey. Clim Res 71:139–153

Lolis CJ, Metaxas DA, Bartzokas A (2008) On the intra-annual variability of atmospheric circulation in the Mediterranean region. Int J Climatol 28:1339–1355

Lolis CJ, Bartzokas A, Lagouvardos K, Metaxas DA (2012) Intra-annual variation of atmospheric static stability in the Mediterranean region: a 60-year climatology. Theor Appl Climatol 110:245–261

Manly BFJ (1986) Multivariate statistical methods: a primer. Chapman & Hall, London

Marsh PT, Brooks HE, Karoly DJ (2009) Preliminary investigation into the severe thunderstorm environment of Europe simulated by the Community Climate System Model 3. Atmos Res 93:607–618

Overland JE, Preisendorfer RW (1982) A significant test for principal components applied to cyclone climatology. Mon Weather Rev 110:1–4

Prezerakos NG, Michaelides SC, Vlassi AS (1990) Atmospheric synoptic conditions associated with the initiation of north-west African depressions. Int J Climatol 10:711–729

Ricard D, Ducrocq V, Auger L (2012) A climatology of the

mesoscale environment associated with heavily precipitating events over a northwestern Mediterranean area. J Appl Meteorol Climatol 51:468–488
Richman MB (1986) Rotation of principal components. J Climatol 6:293–335
Riemann-Campe K, Fraedrich K, Lunkeit F (2009) Global climatology of Convective Available Potential Energy (CAPE) and Convective Inhibition (CIN) in ERA-40 reanalysis. Atmos Res 93:534–545
Rizou D, Flocas HA, Athanasiadis P, Bartzokas A (2015) Relationship between the Indian summer monsoon and the large-scale circulation variability over the Mediterranean. Atmos Res 152:159–169
Rysman JF, Lemaître Y, Moreau E (2016) Spatial and temporal variability of rainfall in the Alps–Mediterranean Euroregion. J Appl Meteorol Climatol 55:655–671
Serra C, Martínez MD, Lana X, Burgueño A (2014) European dry spell regimes (1951–2000): clustering process and time trends. Atmos Res 144:151–174
Tochimoto E, Niino H (2017) Structural and environmental characteristics of extratropical cyclones associated with tornado outbreaks in the warm sector: an idealized numerical study. Mon Weather Rev 145:117–136
WMO (World Meteorological Organization) (1966) Climatic change. Technical Note 79, WMO 195 TP 100, World Meteorological Organization, Geneva
Ziv B, Saaroni H, Alpert P (2004) The factors governing the summer regime of the Eastern Mediterranean. Int J Climatol 24:1859–1871
Ziv B, Saaroni H, Yair Y, Ganot M, Baharad A, Isaschari D (2009) Atmospheric factors governing winter thunderstorms in the coastal region of the eastern Mediterranean. Theor Appl Climatol 95:301–310
Zveryaev II, Hannachi AA (2012) Interannual variability of Mediterranean evaporation and its relation to regional climate. Clim Dyn 38:495–512

Editorial responsibility: Eduardo Zorita, Geesthacht, Germany

Submitted: February 14, 2017; Accepted: August 28, 2017
Proofs received from author(s): September 29, 2017